Measurements of 26 Double Stars with a 254-mm Refractor

Roger C. Ceragioli
University of Arizona, Tucson, AZ; lensbender@msn.com

Abstract

The present paper details measurements made with the author's 254-mm apochromatic refractor during 2022. It describes the full-aperture diffraction grating used to calibrate the objective lens in monochromatic light, and also presents a list of stars measured. Most of these are well-known, frequently measured doubles. A few are "neglected" doubles, *i.e.* pairs not having been measured for several decades.

1. Introduction

The author designed and built a 254-mm f/8 apochromatic refractor in 2020. In late 2022, a program of double-star measurement was commenced. For this purpose, a ZWO ASI290 monochrome camera, together with several color filters, were purchased.

Simultaneously, the author borrowed an Alvan Clark & Sons filar micrometer (constructed *ca.* 1885 and in good working order), restrung it with spider silk, and adapted it for use on the said refractor. The initial goal was to compare measurement modalities of the filar and the CMOS camera. Having calibrated both systems and observed a variety of doubles, the author concluded that he could obtain information more efficiently *via* the CMOS camera than the filar. Hence the filar was laid aside.

2. Equipment and Method of Data Collection for this Report

As indicated, the telescope contains a 254-mm objective lens. The tube assembly is carried on an Astro-Physics™ 1100GTO mounting. The latter allows careful polar alignment and offers a "go to" function, which is very helpful for tracking down faint double stars. In addition, to obtain a good separation of stars, the author uses a Tele-Vue™ 2.5x Power-Mate™ Barlow lens, giving an effective focal length of 5001 mm and focal ratio of 19.7. The Power Mate focuses directly onto the ZWO ASI290 camera, which has square pixels of 2.9 x 2.9 microns in extent.

A critical parameter for telescopic metrology is the image scale (in arcseconds/pixel). This was evaluated by applying a diffraction mask to the objective, consisting of a grating with alternating dark-and-light bars, each 6.35-mm (1/4″) wide. An aluminum plate 1.59-mm (1/16″) thick was mounted on a vertical mill, and rounded to 276 mm (10 7/8″) in outside diameter. Then slots were cut through the plate to produce the "bright bars" of the grating.

Figure 1: Aluminum diffraction grating used to establish the image scale

The dark bars are produced by the uncut aluminum which occults starlight that would (in their absence) pass into the objective lens. The grating was placed over the objective, and the telescope pointed at several bright stars (*e.g.*, Deneb, Capella, *etc.*) to act as point sources.

Over three nights, five stars were imaged in aggregate 67 times through the grating. Their light was filtered by a 7-nm passband ZWO h-alpha filter, placed before the detector. Ten to twelve image files were captured during each observation by means of the software *FireCapture.* Each file contained *ca.* 2000 frames, with exposure times on the order of 5-10 milliseconds. Once capture was completed, the files were opened in *AutoStakkert*. The latter software graded the images, aligned them, and stacked the 5% best frames. The resultant FITS files were then opened with the software *ImagesPlus* and examined. A typical stacked file looked like so:

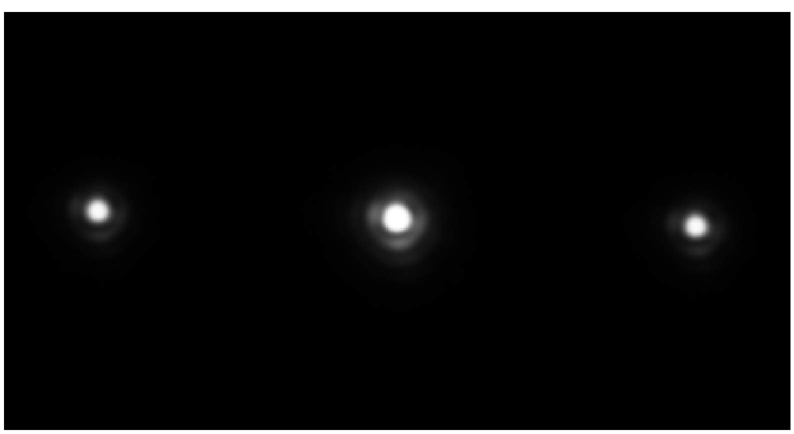

Figure 2: H-alpha diffraction image of Capella through the 254-mm refractor

Having verified the usability of the stacked FITS files, the author then loaded them into the astrometric program, *REDUC*, which determined the pixel coordinates of the Airy disks' centers.

As discussed, *e.g.*, by Maurer (2012) and Cotterell (2015), a diffraction image such as the above consists of a bright, central 0^{th}-order primary star surrounded on either side by two equi-distant 1^{st}-order diffracted images of it. The distance in arcseconds between either 1^{st}-order and 0^{th}-order image is given by the formula:

$$Z = \frac{206{,}265\lambda}{l+d}$$

where Z is the distance in question, *l* and *d* represent the width of the light and dark bars (both 6.35 mm in the present case), and λ is the wavelength of monochromatic light used to take the image (0.0006563 mm for h-alpha). Hence, in the present instance *Z* equals 10.659 arcsec. And the distance from one 1^{st}-order "star" to the other is twice this, namely 21.318 arcsec. Because *Z* is wavelength dependent, it is necessary to filter the starlight entering the camera to obtain sharply defined diffraction "stars." Without a narrow-passband filter, the diffracted images would appear as spectra. With the pixel distance between the 1^{st}-order "stars" established by *REDUC* and the angular distance known from the grating pitch and light wavelength, the image constant can be deduced. *REDUC* calculates this parameter (called "*E*") as 0.1196 arcsec/pixel. And since to smooth the images, *AutoStakkert* resampled them at 2x, the final image-scale constant is one-half as much, namely *E* = 0.0598 arcsec/px.

With the image scale established, it is possible to produce quantitative measurements of double-star separations. The overall method employed was the same as in measuring the diffraction "stars."

That is, having selected a particular double to measure, the author first located it unambiguously. Two methods for this were used. In the first, the epoch J2000 coordinates were taken from the Washington Double Star Catalog (hereafter WDS), or the online resource *Stelle Doppie* (hereafter *SD,* a versatile search engine for the WDS), and fed into the software *Stellarium* (an electronic planetarium program and star atlas) as a search query. The latter then displayed the star-field in question. For brighter doubles (above *ca.* mag. 10.5), *Stellarium* normally shows the double in question, giving both its J2000 as well its current (*i.e.* precessed) coordinates. These latter, in turn, were fed into the AP-1100GTO's hand paddle (used to control slewing) which then moved to the requested position. Of course, the mounting had previously been carefully polar aligned.

The star-field was then examined visually in the finder telescope (75-mm f/5), and scrutinized in comparison with its representation in *Stellarium*. Normally the desired double was seen in the finder telescope near its field center. Other bright stars in the field were also scrutinized with reference to *Stellarium* to verify the double's identity.

The second search method was a variation of this. If the desired double was too faint to register in *Stellarium*, then recourse was had to the *SIMBAD* astronomical database and its visual sky survey. Querying *SIMBAD* with the WDS precise coordinates almost always brought up the correct star. It was then possible to locate the actual star through the finder by reference to *SIMBAD's* image and the surrounding stars. Further confirmation might be had by exposing the full CMOS detector for 5 to 10 seconds and examining the star pattern seen (down to mag. 13). Surrounding fields were sometimes also exposed as part of the confirmation process.

Once the correct star was located and verified, detailed scrutiny ensued to find the companion star. If the latter was clearly seen, then the pair was imaged with *FireCapture* for later stacking and measurement.

As with the diffraction "stars" discussed previously (*cf.* Fig. 2), the author typically acquired ten to twelve files of *ca.* 2000-3000 frames each, exposed for 5-to-100 milliseconds (depending on brightness) with gain and gamma selected to emphasize the stellar Airy disks and (as much as possible) suppress the surrounding Fresnel diffraction rings. The goal was to obtain the best possible stellar "spots" for measurement. To this end, the author found it advantageous to mask the circular aperture of his objective lens with a full-sized hexagonal mask. This well-known technique of double-star observing tends to suppress the Fresnel rings and divert their light into six thin and faint diffraction spikes around the Airy disk. These methods were constantly employed to obtain the most measurable images.

The resultant files were then graded and stacked in *AutoStakkert* and measured in *REDUC*. Other methods of image selection were also tried, such as grading and selecting a small number of "lucky images," which approximate to diffraction limited. But the statistical scatter of measurements was then much greater and the averages appeared no better than with the stacking procedure outlined.

Position angles were calibrated and measured per the instructions of F. Losse in his user's guide to *REDUC* (*i.e.*, *via* the well-known "star-drift" or "trail" method).

3. Data Acquired

The following tables summarize the data, and their probable errors. In Table 1, we have numbers derived from the WDS for comparison. From left to right, we have in the first column the WDS 9-digit identifier. In column two appears the discoverer's code and catalog number. The third and fourth columns present the WDS-listed magnitudes of the primary and secondary stars. The fifth column gives the magnitude difference. The sixth and seventh columns list the position angle (θ) and separation (ρ) of the stars, according to the latest observation contained in the WDS, measured in the year specified in the eighth and last column.

Table 1. WDS data on the doubles measured.

WDS ID	Name	M1	M2	ΔM	WDS θ	WDS ρ	Year
21069+3845	STF2758AB	5.20	6.05	0.85	154°	31.9″	2021
21330+2043	STF2804AB	7.70	8.04	0.34	359°	3.3″	2019
21582+8252	STF2873AB	7.00	7.47	0.47	66°	13.8″	2017
22029+4439	BU694AB	5.71	7.76	2.05	8°	1.0″	2020
22038+6438	STF2863AB	4.45	6.40	1.95	274°	8.1″	2020
23075+3250	STF2978	6.35	7.46	1.11	145°	8.3″	2018
22441+3928	STF2942AB	6.18	8.94	2.76	278°	2.9″	2016
23078+3947	STF2979	7.92	9.99	2.07	229°	2.8″	2016

23104+4901	STF2987	7.42	10.41	2.99	150°	4.2″	2017
23186+6807	STF3001AB	4.97	7.28	2.31	223°	3.4″	2020
23228+2034	STF3007AB	6.74	9.78	3.04	92°	5.5″	2017
23595+3343	STF3050AB	6.46	6.72	0.26	343°	2.5″	2021
00026+5942	MLB106AB	11.36	11.60	0.24	43°	2.2″	1998
00094+4232	COU1046	9.98	11.60	1.62	27°	2.4″	1997
00491+5749	STF60AB	3.52	7.36	3.84	326°	13.6″	2020
01001+4443	STF79	6.04	6.77	0.73	195°	7.9″	2018
01004+3228	ES317	9.20	9.40	0.20	194°	7.0″	2016
01467+3310	STF158AB	8.96	9.40	0.44	272°	2.2″	2018
02124+3018	STF227	5.26	6.67	1.41	68°	4.0″	2019
02291+6724	STF262AB	4.63	6.92	2.29	230°	2.9″	2017
02291+6724	STF262AC	4.63	9.05	4.42	117°	6.7″	2015
02300+5715	BU1172AB	8.70	11.10	2.40	237°	1.7″	1967
03122+3713	STF360	8.02	8.29	0.27	125°	2.9″	2019
03443+3217	BU535	3.91	6.70	2.79	20°	1.1″	2015
03470+4126	STF443AB	8.20	8.82	0.62	55°	6.6″	2020
04524+5124	HU553	8.96	11.20	2.24	82°	3.1″	1964

Table 2 presents the author's measured data. Columns one and two reprise the WDS ID and discoverer codes. Columns three and four present the author's measured position angle and separation. These are averages of all the stacked images. Column five lists the Julian epoch (JE) of observation. And columns six and seven give the number of images stacked, and the number of nights on which the star was observed. When more than one night is indicated, the θ, ρ, and the JE are averages of all the individual stacked images.

Table 2. Author's measurements.

WDS ID	Name	Obs. θ	Obs. ρ	JE	#Ims	#Nts
21069+3845	STF2758AB	153.5°	31.99″	2022.85	10	1
21330+2043	STF2804AB	359.4°	3.41″	2022.85	11	1
21582+8252	STF2873AB	65.4°	13.70″	2022.85	12	1
22029+4439	BU694AB	7.9°	0.96″	2022.90	24	1
22038+6438	STF2863AB	274.5°	7.88″	2022.90	19	2
23075+3250	STF2978	144.3°	8.29″	2022.90	12	1
22441+3928	STF2942AB	277.2°	2.81″	2022.90	12	1
23078+3947	STF2979	228.9°	2.78″	2022.85	10	1
23104+4901	STF2987	149.0°	4.16″	2022.97	12	1
23186+6807	STF3001AB	223.8°	3.44″	2022.85	11	1
23228+2034	STF3007AB	92.1°	5.85″	2022.97	12	1
23595+3343	STF3050AB	343.3°	2.58″	2022.85	12	1
00026+5942	MLB106AB	42.3°	2.15″	2022.96	19	2
00094+4232	COU1046	27.1°	2.42″	2022.95	24	2

00491+5749	STF60AB	327.2°	13.41″	2022.94	9	1
01001+4443	STF79	193.9°	7.88″	2022.90	11	1
01004+3228	ES317	194.3°	7.06″	2022.97	7	1
01467+3310	STF158AB	271.7°	2.24″	2022.94	10	1
02124+3018	STF227	67.2°	4.01″	2022.97	11	1
02291+6724	STF262AB	230.8°	2.98″	2022.97	12	1
02291+6724	STF262AC	116.5°	6.93″	2022.97	12	1
02300+5715	BU1172AB	237.0°	1.72″	2022.98	24	2
03122+3713	STF360	124.3°	2.98″	2022.96	11	1
03443+3217	BU535	20.5°	1.02″	2022.90	8	1
03470+4126	STF443AB	56.6°	6.81″	2022.98	9	1
04524+5124	HU553	83.1°	2.94″	2022.96	10	1

Table 3 indicates the statistical errors, specifying the standard deviations (SD) of position angles (θ) and separations (ρ), together with their standard errors of the mean (SEM), derived from the author's measures. The standard deviations come directly from *REDUC*. The standard errors were computed by the author. Where the double star in question was observed on more than one night, these are averages of the individual numbers. Following Table 3, for illustration there are presented several representative stacked images used in the measurements.

Table 3. Measurement errors.

WDS ID	Name	θ SD	θ SEM	ρ SD	ρ SEM
21069+3845	STF2758AB	0.02	0.006	0.02	0.006
21330+2043	STF2804AB	0.09	0.027	0.01	0.003
21582+8252	STF2873AB	0.08	0.023	0.04	0.012
22029+4439	BU694AB	1.26	0.257	0.03	0.006
22038+6438	STF2863AB	0.15	0.034	0.03	0.007
23075+3250	STF2978	0.07	0.020	0.02	0.006
22441+3928	STF2942AB	0.28	0.081	0.03	0.009
23078+3947	STF2979	0.15	0.047	0.01	0.003
23104+4901	STF2987	0.38	0.110	0.03	0.009
23186+6807	STF3001AB	0.19	0.057	0.02	0.006
23228+2034	STF3007AB	0.48	0.139	0.05	0.014
23595+3343	STF3050AB	0.11	0.032	0.01	0.003
00026+5942	MLB106AB	0.36	0.083	0.06	0.014
00094+4232	COU1046	0.28	0.057	0.02	0.004
00491+5749	STF60AB	0.16	0.053	0.04	0.013
01001+4443	STF79	0.09	0.027	0.01	0.003
01004+3228	ES317	0.09	0.034	0.02	0.008
01467+3310	STF158AB	0.19	0.060	0.01	0.003
02124+3018	STF227	0.22	0.066	0.04	0.012

02291+6724	STF262AB	1.27	0.367	0.06	0.017
02291+6724	STF262AC	0.29	0.084	0.04	0.012
02300+5715	BU1172AB	1.58	0.323	0.07	0.014
03122+3713	STF360	0.49	0.148	0.06	0.018
03443+3217	BU535	1.52	0.537	0.04	0.014
03470+4126	STF443AB	0.16	0.053	0.03	0.010
04524+5124	HU553	0.21	0.066	0.02	0.006

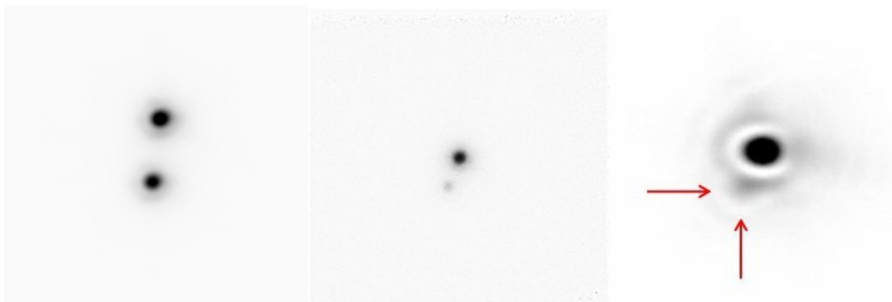

Figure 3: Selected images of doubles. From left to right: STF2804AB; COU1046; and the difficult pair BU535 (with arrows pointing to the secondary)

4. Discussion

It will be useful, in addition, to show the residuals of the author's measurements from the last WDS published data, as well as from the orbital ephemeris (if a published orbit exists), so that the reader may assess the validity of the present results. To that end, Table 4 is provided. The first and second columns are as in the previous tables. The third and fourth give the residuals, showing the author's observations minus the most recent WDS data, and the author's work minus the current (2023) ephemeris position, respectively. The ephemerides come from Matson, *et al.*, *Sixth Catalog of Orbits of Visual Binary Stars*. The fifth column ("Ref.") references the published orbit that generated the ephemeris in question.

Table 4. Residuals from WDS and 2023 Ephemerides.

WDS ID	Name	Δ from WDS (θ, ρ)	Δ from 2023 (θ, ρ)	Ref.
21069+3845	STF2758AB	-0.5°, 0.09″	-0.2°, 0.02″	Izm 2019
21330+2043	STF2804AB	0.4°, 0.11″	-0.2°, 0.05″	Izm 2019
21582+8252	STF2873AB	-0.6°, -0.10″	0.0°, -0.02″	Izm 2019
22029+4439	BU694AB	-0.1°, -0.04″	N/A	N/A
22038+6438	STF2863AB	0.5°, -0.22″	0.5°, -0.24″	Izm 2019
23075+3250	STF2978	-0.7°, -0.01″	N/A	N/A
22441+3928	STF2942AB	-0.8°, -0.09″	N/A	N/A
23078+3947	STF2979	-0.1°, -0.02″	-0.1°, 0.02″	Izm 2019

23104+4901	STF2987	-1.0°, -0.04″	-0.3°, -0.03″	Izm 2019
23186+6807	STF3001AB	0.8°, 0.04″	0.1°, -0.01″	Izm 2019
23228+2034	STF3007AB	0.1°, 0.35″	-3.0°, 0.05″	Tok 2016d
23595+3343	STF3050AB	0.3°, 0.08″	-0.4°, 0.05″	Izm 2019
00026+5942	MLB106AB	-0.7°, -0.05″	N/A	N/A
00094+4232	COU1046	0.1°, 0.02″	N/A	N/A
00491+5749	STF60AB	1.2°, -0.19″	-0.4°, -0.07″	Sca 2015c
01001+4443	STF79	-1.1°, -0.02″	-0.1°, -0.02″	FMR 2020c
01004+3228	ES317	0.3°, 0.06″	N/A	N/A
01467+3310	STF158AB	-0.3°, 0.04″	-0.6°, 0.14″	Izm 2019
02124+3018	STF227	-0.8°, 0.01″	-0.8°, 0.10″	FMR 2020c
02291+6724	STF262AB	0.8°, 0.08″	2.9°, -0.07″	Tok 2021b
02291+6724	STF262AC	-0.5°, 0.23″	N/A	N/A
02300+5715	BU1172AB	0.0°, 0.03″	N/A	N/A
03122+3713	STF360	-0.7°, 0.08″	-0.4, 0.01″	Tok 2020i
03443+3217	BU535	0.5°, -0.08″	N/A	N/A
03470+4126	STF443AB	1.6°, 0.21″	-0.1°, 0.04″	Izm 2019
04524+5124	HU553	1.1°, -0.16″	N/A	N/A

A few comments may be helpful. As can be seen, in most cases the residuals are small. Where the position angles differ by > 1.0°, or the separations by > 0.1″, this may be due to errors in the author's measurements (for example, because of inadequate position angle calibration), or it may be due to limitations in the last WDS published position, or problems with the published orbit, or lastly because of actual motion of the secondary star in the interval between the author's and the last published WDS measurements. Examples include HU553 (with differences of 1.1° and -0.16″), which was last measured in 1964; and perhaps MLB106AB (with differences of -0.7° and -0.05″), which was last measured in 1998. Here the differences could indicate real motion. Whereas, with STF2987, 3001AB, 60AB, STF79, and 443AB, the author's measurements diverge from the latest published data but agree more closely with the orbital ephemerides by Izmailov, Scardia, and Rica Romero. This might point to limitations with the most recent published observations. On the other hand, divergences in the cases of STF3007AB and 262AB may point to problems with the published orbits. And lastly, STF2863AB and 227 may point to errors in the author's data. In future, the author plans to observe all pairs on multiple nights and take 3-5 star trails each time for averaging.

It will also be noted that a handful of doubles (*e.g.*, BU1172AB, BU535, *etc.*) show large standard deviations, especially in position angle (θ). This is because with these stars it was necessary (on account of the secondaries' relative faintness and closeness to their primaries) to measure them "manually," that is, to place fitting boxes around the components one by one, since the *REDUC* algorithm could not in all cases dependably distinguish both stars in the pairs. The manual element introduces greater variance into the measuring process.

5. Conclusions

The above measurements executed in the last months of 2022 appear reasonable in general, and perhaps worthy of inclusion in the WDS dataset. The author hopes to continue making measurements, with an emphasis on pairs not examined since the year 2000, which also lie within the range of his instrumentation.

6. Acknowledgments

This research has made use of the Washington Double Star Catalog maintained at the U.S. Naval Observatory. The author wishes to thank the USNO. Also, G. Sordiglioni for use of *Stelle Doppie*; F. Losse for *REDUC*; E. Kraaikamp for *AutoStakkert*; T. Edelmann for *FireCapture*; and M. Unsold for *ImagesPlus*.

The author also acknowledges and thanks *Stellarium*, and the SIMBAD database. Finally, the author expresses his gratitude to his friends D. Schmidt for advise regarding CCD imaging, and J. Briggs for use of his Alvan Clark & Sons filar micrometer.

References

Cotterell, J.D. (2015). “Calibrating the Plate Scale of a 20 cm Telescope with a Multiple-Slit Diffraction Mask.” *Journal of Double Star Observations*, 11(4), 387-389.

Losse, F., “REDUC Tutorial,” (V5.34). Retrieved from http://www.astrosurf.com/hfosaf/reduc/tutorial.htm

Mason, B.D. *et al.*, “Washington Double Star Catalog.” Retrieved from http://www.astro.gsu.edu/wds/

Matson, R.A., *et al.*, *“Sixth Catalog of Orbits of Visual Binary Stars.”* Retrieved from http://www.astro.gsu.edu/wds/orb6.html

Maurer, A. (2012). “The Diffraction Grating Micrometer.” In R.W. Argyle (ed.), *Observing and Measuring Visual Double Stars*, (Springer), 183-193.

……………………………………..

About the author: Roger Ceragioli works as an optical engineer at the Richard F. Caris Mirror Lab, University or Arizona, Tucson, USA. His expertise is in optical fabrication and design, and he is in charge of diamond generating operations on the Giant Magellan Telescope’s primary mirrors. He holds a Ph.D. from Harvard University.